Received: 29 May 2020 | Revised: 19 August 2020 | Accepted: 21 August 2020

DOI: 10.1096/fj.202001357R

RESEARCH ARTICLE

THE FASEB JOURNAL

Exposing human primary dermal fibroblasts to particulate matter induces changes associated with skin aging

Wil J. Reynolds[1] | **Peter S. Hanson**[2] | **Adam Critchley**[3] | **Ben Griffiths**[3] | **Bhaven Chavan**[4] | **Mark A. Birch-Machin**[1]

[1]Dermatological Sciences, Translational and Clinical Research Institute, Newcastle University, Newcastle upon Tyne, UK

[2]Campus for Ageing and Vitality, Translational and Clinical Research Institute, Newcastle University, Newcastle upon Tyne, UK

[3]Royal Victoria Infirmary, Newcastle upon Tyne, UK

[4]Croda Europe Ltd, Snaith, UK

Correspondence
Mark Birch-Machin, Dermatological Sciences, Translational and Clinical Research Institute, Newcastle University Medical School, Newcastle upon Tyne, NE2 4HH, UK.
Email: mark.birch-machin@ncl.ac.uk

Funding information
UK Research and Innovation/Biotechnology and Biological Sciences Research Council

Abstract

With a large proportion of the world's population living in areas where air quality does not meet current WHO guidelines, combined with the knowledge that pollutants can interact with human skin, it is now of even greater importance that the effects of air pollutant exposure on human skin be investigated. To evaluate the damaging effects of a known component of air pollution (particulate matter) on human primary dermal fibroblasts. These studies were undertaken by exposing primary human dermal fibroblasts to different concentrations of particulate matter and analyzing the effects over time using resazurin reduction assays. Immunofluorescence microscopy was used to determine if particulate matter caused activation of the aryl hydrocarbon receptor, and phosphorylation of histone H2AX, a known marker of double-strand DNA breaks. Dot blotting was also used to analyze expression changes in secreted MMP-1, MMP-3, and TGFβ. Particulate matter was found to dose-dependently increase cellular viability, activate the aryl hydrocarbon receptor, increase double-strand DNA breaks, and increase the expression of MMP-1, MMP-3, and TGFβ. With the potential of air pollutants such as particulate matter to not only modulate the expression of proteins implicated in skin aging, but also affect cells at a genetic level, brings a pressing need for further investigation so protective strategies can be implemented.

KEYWORDS

aging, oxidative stress, pollution

1 | INTRODUCTION

Global increases in air pollutant levels have always existed as a major health concern, however, it is only with research conducted in the last decade that new modes of action for these pollutants to harm have surfaced. Alongside the already established inhalation route, dermal absorption is now believed to be an additional route for various pollutants to enter internal systems and inflict damage, the mechanisms of which are now the focus of many research groups.[1,2] The World Health Organization (WHO) 2018 report states that 91% of the world's population live in areas where the air quality exceeds WHO air

Abbreviations: AhR, aryl hydrocarbon receptor; DMSO, dimethyl sulfoxide; DSBs, double strand DNA breaks; MMP, matrix metalloproteinase; PAHs, polycyclic aromatic hydrocarbons; PM, particulate matter; ROS, reactive oxygen species; TGFβ, transforming growth factor beta.

quality guideline limits, and of even greater concern over 4.2 million people die annually as a result of exposure to ambient air pollution; this highlights an urgent need for investigation.[3] Ambient air pollutants can come in a various forms with each being classified as either a primary or secondary pollutant; primary pollutants are those that are emitted directly from a source, secondary pollutants are those formed when primary pollutants react together in the atmosphere. One example of a primary pollutant that has been implicated in the damage of skin structure and function is particulate matter (PM).[4] PM is a complex mixture of microscopic particles and liquid droplets suspended in air, which can originate from a number of different anthropogenic sources including motor vehicle emissions, open fires, and power plant byproducts, but also natural sources such as volcanoes and pollen.[5] It is suggested that PM can exert their skin damaging effects through two different formats; the first is the effects exerted through the particle itself, with their large surface area making them highly reactive toward biological surfaces (such as skin), where they can penetrate transepidermally, or through hair follicles.[6-8] Their ability to penetrate deeper into the skin seems to be augmented by the presence of a compromised skin barrier, this impaired integrity can be seen in multiple skin conditions (including psoriasis and atopic dermatitis), but also with increasing age.[9,10] The second is their ability to act as carriers for other organic chemicals, such as polycyclic aromatic hydrocarbons (PAHs), which are capable of adsorbing on to the surface of PM and exerting their own damaging effects.[11] Inhaled PAHs have also been shown to cross epithelial barriers from the pulmonary alveoli and enter systemic circulation, giving them a potential alternate route to reach the deeper skin layers.[12] When PM/PAHs passively diffuse across a cell membrane they are capable of binding to the aryl hydrocarbon receptor (AhR), subsequently, AhR translocates into the nucleus where it heterodimerizes to the AhR nuclear translocator (ARNT) and dissociates from the complex. This heterodimer can then bind to DNA sequences in promoter regions of target genes known as xenobiotic response elements (XREs), and initiate transcription of these target genes, including cytochrome P450s (CYP) 1A1, 1A2, and 1B1.[13-15] Once translated these xenobiotic metabolizing enzymes can convert PM to quinones, these redox-cycling compounds have the ability to produce reactive oxygen species (ROS) and are believed to be the main culprit of a broad spectrum of not only PM-induced damage (Figure 1).[6] Increases in ROS in skin cells have also been observed after exposure to other environmental agents such as ultraviolet radiation and ozone.[16,17]

Ambient air pollutants like PM represent a global health risk, and have already been implicated as a risk factor for various cancers, cardiovascular and pulmonary diseases.[18,19] In recent years the role of PM in skin aging has been brought into question, with a number of studies showing a significant correlation between air pollution and extrinsic skin aging.

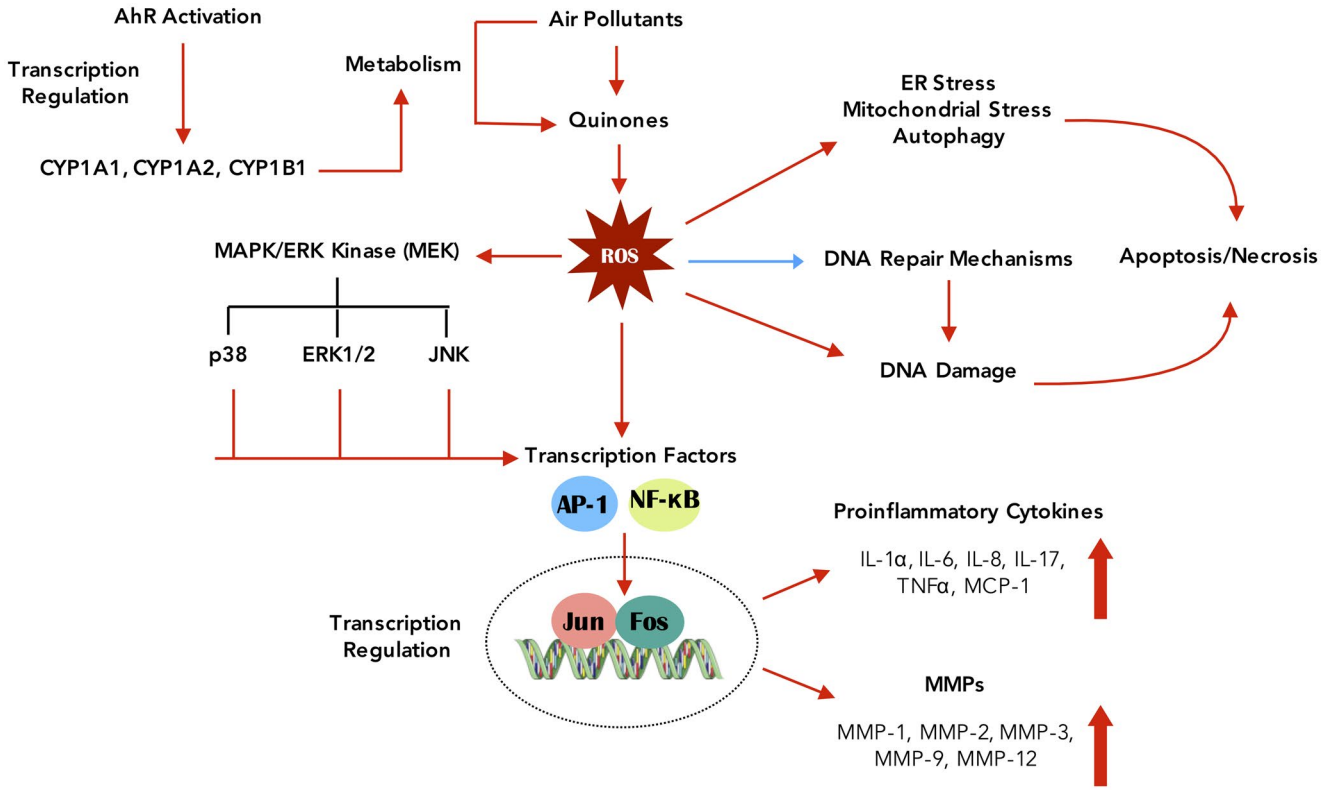

FIGURE 1 PM-induced damage mechanisms. Possible mechanisms that PM can use to influence cellular processes and modulate expression of proteins in dermal fibroblasts

One epidemiological study showed that increased PM exposure from traffic was associated with a 20% increase in pigment spots on the forehead and cheeks, with another showing that smokers were almost five times more likely to have facial wrinkles than nonsmokers.[6,20] Alongside premature skin aging, pollutants have also been implicated in the induction and/or advancement of a number of different dermatological conditions, including but not limited to eczema, atopic dermatitis, and even cancers.[21]

The development of protective strategies for extrinsic skin aging has gained momentum over recent years, this is because the factors causing extrinsic aging are more easily modified than the genetic factors causing intrinsic aging. For this reason, the anti-aging product market is ever-expanding, with the global market worth $250 billion in 2016 and set to rise to $331 billion by 2021.[22] With age, the skin undergoes progressive structural and functional deterioration, and with it being the most visible organ, signs of skin aging can greatly impact a person's self-esteem. Since fibroblasts in the dermal layer are responsible for producing the extracellular matrix (ECM) proteins that provide the skin with its structural and elastic properties (eg, collagen and tropoelastin), they are responsible for the majority of characteristic features of skin aging. This is owing to the fact that the fibroblast functionality declines with age, this includes a reduction in their ECM synthesizing capacity, and enhanced production of matrix metalloproteinases (MMPs) that are capable of degrading ECM components, resulting in compromised skin integrity and the appearance of skin aging.[23] With this in mind, the damaging effects that different types of air pollutants have on human skin is something that needs further investigation, as current research in this area is still limited. This study investigates some of the damaging effects of a known component of air pollution (particulate matter) on primary human dermal fibroblasts.

2 | MATERIALS AND METHODS

Unless otherwise stated, all materials and reagents were purchased from Sigma-Aldrich (Poole, UK) and were of molecular or analytical grade.

2.1 | Preparation of particulate matter

A master stock of SRM 1649b aka "urban dust particulate matter" (PM) was purchased from the National Institute of Standards and Technology (NIST), and prepared at a concentration of 50 mg/mL in dimethyl sulfoxide (DMSO). Prior to the preparation of culture treatments, the master stock was sonicated in a sonic bath for 1 h at 25°C with regular vortexing to avoid any agglomeration of particles. After the PM was added to fibroblast medium, experiments were performed within 1 h of stock preparation to limit any variability in solution composition.

2.2 | Cell culture

Primary human dermal fibroblasts were isolated from human female breast tissue, obtained from the Royal Victoria Infirmary, Newcastle, UK, following standardized methods. Fibroblasts were maintained in culture medium (Advanced DMEM medium supplemented with 10% (v/v) of fetal bovine serum (FBS), 1% (v/v) of Glutamax, and 100 U of Penicillin/Streptomycin). For all experiments, fibroblasts were seeded on tissue culture-treated plates at a density of 20 000 cells/cm^2 and treated when they reached 70% confluence. For secretory protein analysis, cells were treated with fresh PM in fibroblast medium every 2-3 d (8 & 24 h exposures consisted of one treatment, 4 d consisted of two treatments, and 7 d consisted of three treatments). Cell medium was changed to FBS-free medium for 8-24 h prior to harvesting, this is so FBS would not interfere with antibody validation using Western blotting.

2.3 | Resazurin reduction viability assay

Cells were seeded into a 48-well plate at a density of 20 000 cells/well and cultured for 48 h before adding 350 μL of resazurin medium (10 μg/mL resazurin in fibroblast medium) and incubating for 2 h at 37°C. After this incubation, 100 μL of the medium was transferred to each well of a 96-well plate in duplicate and read in a Tecan Infinite 200 Pro M Nano+ (ex = 530, em = 590). This background reading allowed for any differences in cellular viability to be seen on a well by well basis, and factored in any differences in cell seeding. Following this 350 μL of treatment medium was added to each well and after each incubation time, the medium was aspirated, replaced with 350 μL of freshly sterile filtered resazurin medium and incubated for 2 h at 37°C. After this incubation, 100 μL of medium was transferred to each well of a 96-well plate in duplicates and read in a Tecan Infinite 200 Pro M Nano+ (ex = 530, em = 590). Cell seeding number and resazurin concentration were first optimized prior to experiments. Hydrogen peroxide (1.96 μM) was used as a positive control for cell death to ensure cells were not immortalized.

2.4 | Immunocytochemistry

After incubating with PM for 24 h, cells were washed with phosphate-buffered saline (PBS), before fixing with either

3.7% (w/v) paraformaldehyde and permeabilized with 70% (v/v) ethanol for γ-H2AX, or with 80% (v/v) acetone for AhR. After cells were washed with PBS and blocked with 5% normal goat serum in PBS, cells were incubated with γ-H2AX (1/1000, Cell Signaling Technology) or AhR (1/1000, GeneTex) in antibody incubation buffer (1% Bovine Serum Albumin, 0.2% Triton-X100 in PBS). After overnight incubation at 4°C, cells were washed with PBS, followed by 1 h incubation of fluorescent IgG-conjugated secondary antibody (Alexa Fluor 594). Cells were once again washed before counterstaining with DAPI solution (300 nM) for 5 min at room temperature, washed and mounted in Prolong Glass Antifade mountant. Cells were imaged using the Zeiss Axioplan 2 microscope (Zeiss, Germany), for quantification 300+ cells were analyzed (around 25-30 fields of view). Integrated density (the product of mean gray value and area) was used as a measure for the total amount of protein in a given region of interest.

2.5 | Dot blotting

Samples were prepared to a concentration of 0.1 μg/μL in Orange G Sample Buffer (0.2% w/v Orange G, 62.5 mM Tris-HCl, 20% v/v 10% SDS, and 25% v/v glycerol) and NuPAGE Sample Reducing Agent (Invitrogen, UK), before heating at 70°C for 10 min. Vacuum-assisted 96-well Bio-dot Microfiltration apparatus (BioRad) was used to pull protein samples onto a 0.2 μm nitrocellulose membrane (Amersham) which was assembled on top of thick filter paper (0.5 cm) in between a sealing gasket and sample template. Membranes and filter paper were soaked in TBS before loading 50 μL of protein sample per well. After loading each well was washed with another 100 μL of TBS, before the membrane was dried and fixed in 70% of methanol for 20 min under agitation. The membrane was probed with Revert Total Protein Stain (Licor, UK) as a normalization factor for protein quantification analysis, and imaged using the Odyssey Fc Dual-Mode Imaging System. Immunodetection was performed by first blocking the membrane in Odyssey blocking buffer (Licor, UK) before incubating the membrane with primary antibody (anti-MMP-1, R&D; anti-MMP-3, R&D, anti-TGFβ1/2/3, R&D) overnight at 4°C. This was followed by 1 h incubation with the appropriate species IRDye 800CW, before imaging and quantifying using the Odyssey Fc Dual-Mode Imaging System.

2.6 | Statistical analysis

D'Agostino-Pearson omnibus was used to test for Gaussian distribution. Two-way ANOVA corrected for multiple comparisons using the Dunnett's test, or Kruskal-Wallis corrected for multiple comparisons using the Dunn's test, were performed based on normality test results (see figure legends).

3 | RESULTS

3.1 | PM induces increases in cellular viability

Changes in dermal fibroblast viability after exposure to a range of PM concentrations over several different incubation times were evaluated by analyzing the extent of resazurin reduction.

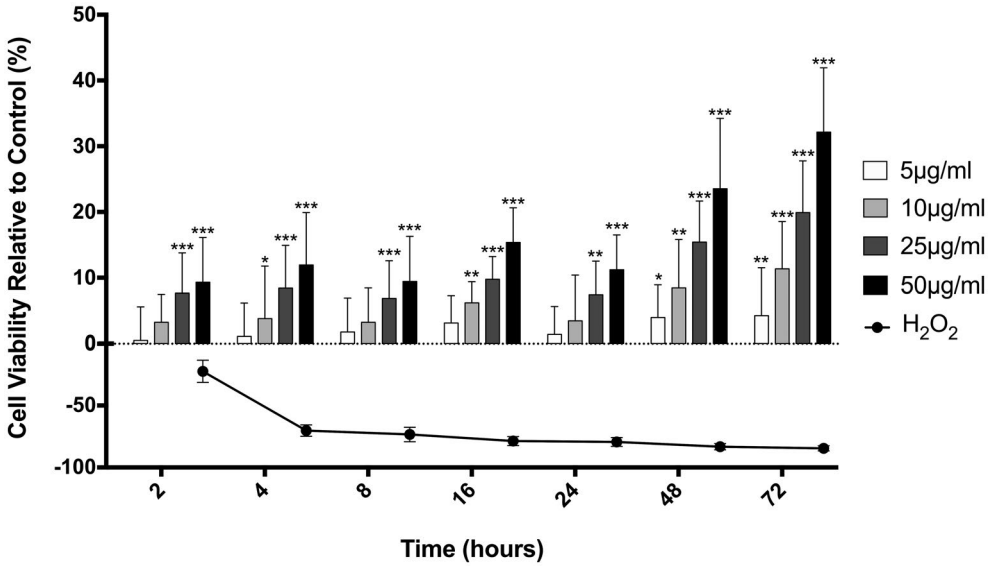

FIGURE 2 PM-induced increases in dermal fibroblast viability using resazurin reduction viability assays. Graph shows mean + SD and is based on dermal fibroblasts isolated from three separate donors, with each donor consisting of triplicate experiments (n = 3). Values are normalized to individual background reading before being presented as the percentage change after subtracting the DMSO control group. Two-way ANOVA was performed and corrected for multiple comparisons using the Dunnett's Test. *$P < .05$, **$P < .01$, ***$P < .001$

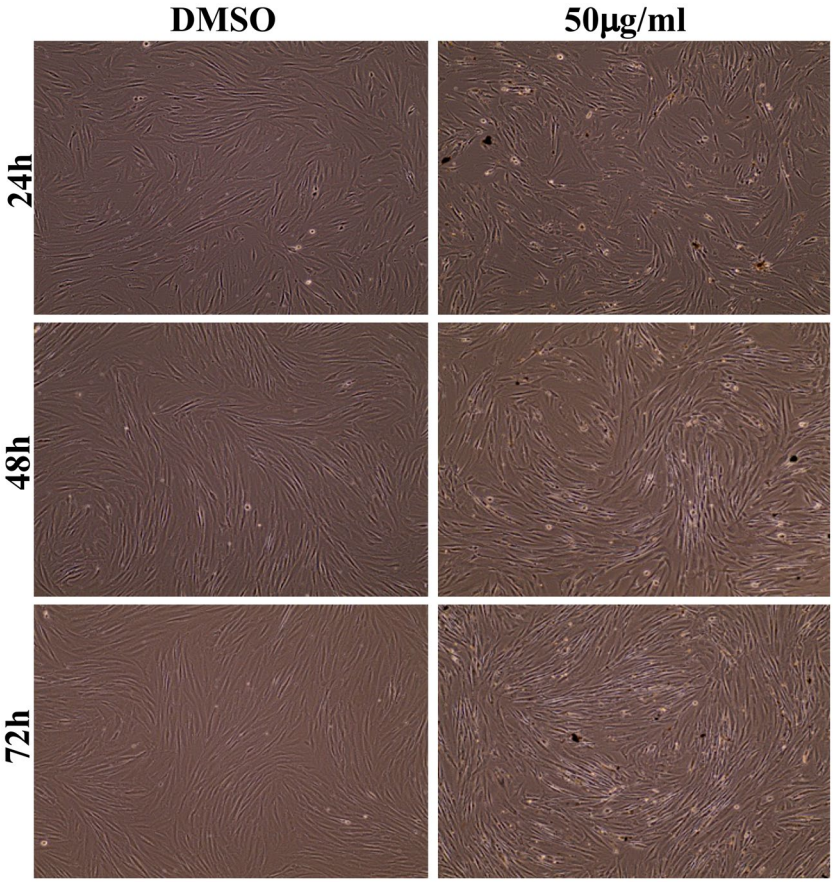

FIGURE 3 PM-induced increases in dermal fibroblast proliferation rate. Fibroblasts treated with 50 µg/mL showed an increased cell density compared to the DMSO vehicle control group, this is more apparent at longer exposure times

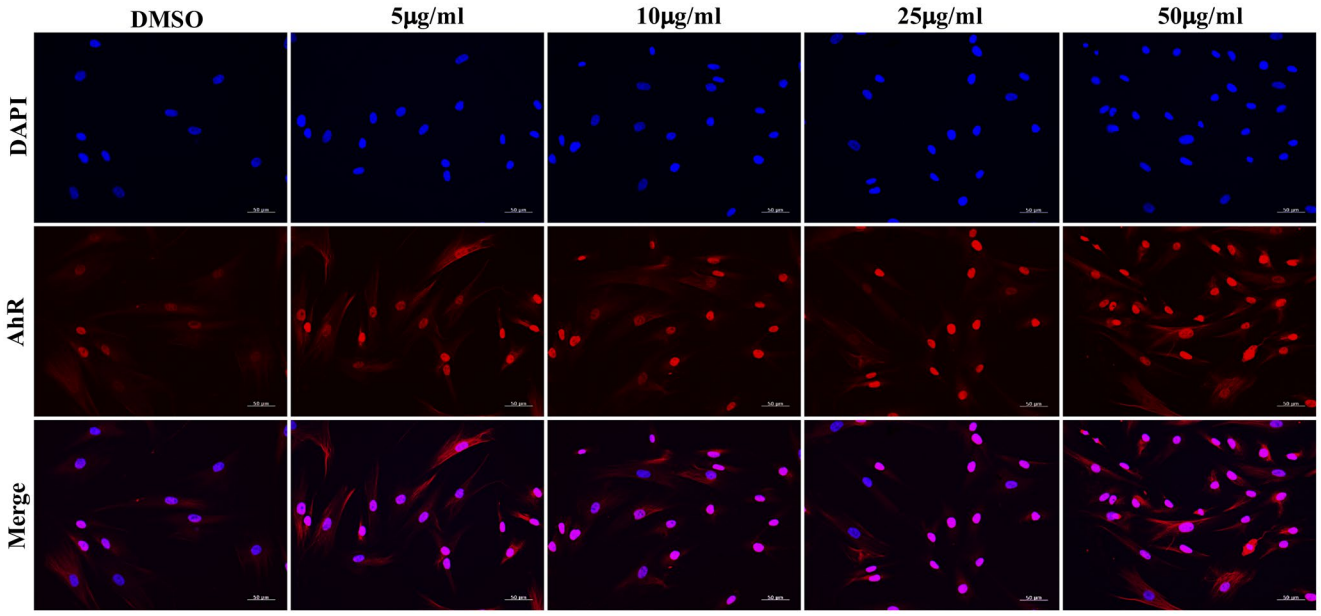

FIGURE 4 Effect of PM on AhR activation in dermal fibroblasts after 24 h of exposure. Dermal fibroblasts were treated with DMSO (vehicle control) or different concentrations of PM for 24 h and fixed. Cells were then stained with anti-AhR antibody and counterstained with 4,6-diamidino-2-phenylindole (DAPI), before being visualized with fluorescence microscopy

Resazurin is reduced to fluorescent resorufin in proportion to the metabolic activity of a cell population, indicating an increase in cell number, mitochondrial number, or mitochondrial activity.[24] Exposing dermal fibroblasts to PM caused an increase in cellular viability in a dose-dependent manner. From 2-24 h, cells showed minor increases in cellular viability with an average percentage increase of 1.6%, 4%, 8%, and 11.4% for 5, 10, 25, and 50 µg/mL, respectively (Figure 2). Between

24 and 72 h, the cellular viability increased more notably, with an average percentage increase of 4.2%, 10%, 17.7%, and 27.8% for 5, 10, 25, and 50 μg/mL, respectively. After observation using light microscopy, it appeared PM increased the fibroblast proliferation rate, however, mitochondrial changes cannot be discounted especially given the known oxidative properties of the PM mixture (Figure 3).[25] Fibroblasts also seemed to have decreased cytoplasmic volume, assuming a thinner, more spindle-like morphology after PM exposure.

3.2 | PM activates AhR

Immunocytochemistry was used to analyze AhR intracellular distribution in dermal fibroblasts after incubation with various concentrations of PM for 24 h. DMSO treated fibroblasts showed a low level of both cytoplasmic and nuclear AhR (Figure 4). Upon treatment with PM, the proportion of cells with a higher intensity of nuclear AhR increased in a concentration-dependent manner, which coincided with a parallel reduction in the intensity of cytoplasmic AhR. The nuclear AhR intensity of a small percentage of cells did not change with PM treatment, therefore, quantification of nuclear AhR was done on a cell by cell basis using integrated density to take into account any changes in nuclei size (Figure 5A). With each donor having slightly different baselines of nuclear AhR, it was also of interest to analyze AhR activation for each donor separately. As seen in Figure 5B, the extent of PM-induced AhR activation relative to the DMSO treated control seems to be very similar between all three donors. The mean increase between the three donors was 5.2%, 9.3%, 13.5%, and 21.2% with a relative standard deviation of 1.8%-4% for 5, 10, 25, and 50 μg/mL, respectively.

3.3 | PM induces phosphorylation of H2AX

After 24 h of exposure to different concentrations of PM, the number of nuclear foci was analyzed using immunocytochemistry. Nuclear foci correspond to the phosphorylation of histone H2AX which occurs immediately after double-strand DNA breaks (DSBs). Figure 6 shows that a higher percentage of the cell population had a higher number of H2AX-stained nuclear foci after PM treatment in a dose-dependent manner. The analysis of the results for all three donors confirms that PM dose-dependently increases the number of H2AX-stained nuclear foci, as shown in Figure 7A. It is also important to note that histone H2AX is also phosphorylated during the S phase of the cell cycle in proliferating cells as the replicative forks collapse during DNA synthesis.[26] This explains the smaller number of phosphorylated H2AX nuclear foci present in the DMSO-treated control cells. Due to the presence of phosphorylated H2AX in untreated controls it was important to analyze any differences in DSB induction between donors. Figure 7B shows the extent of PM-induced H2AX phosphorylation for each donor separately. Donors 2 and 3 followed a very similar percentage increase across PM concentrations, with a mean increase of 56.4%, 66%, 87.3%, and 149.5% with a relative standard deviation of 0.2%-9.4% for 5, 10, 25, and 50 μg/mL, respectively. However, in Donor 1 PM induced a larger increase in DSBs from the lower concentration of 10 μg/mL, with increases of 62.8%, 122.9%, 151.3%, and 171.3% for 5, 10, 25, and 50 μg/mL, respectively.

3.4 | PM increases expression of MMP-1 & MMP-3

Antibody specificity for MMP-1 and MMP-3 was confirmed with Western blotting, before analysis of secretory MMP expression in dermal fibroblasts after PM treatment using dot

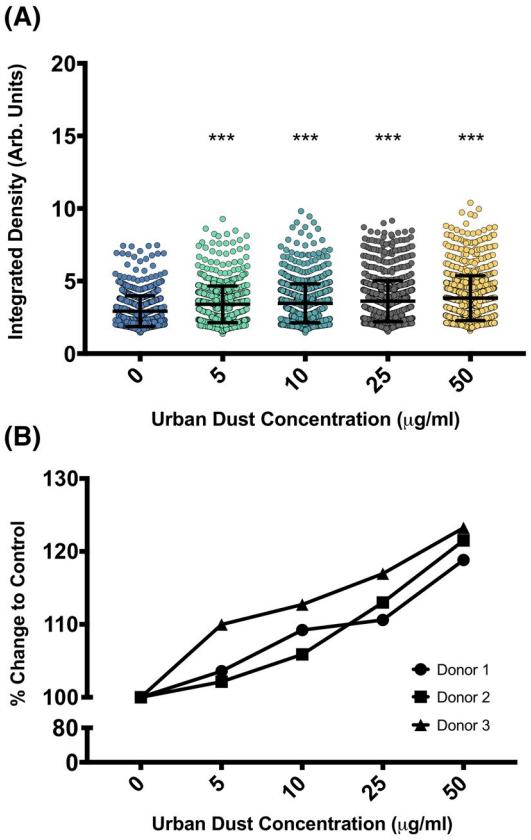

FIGURE 5 Activation of AhR by PM. The intensity of AhR staining for each individual cell nuclei for all three donors after PM exposure is shown in Figure 5A (n = 3). The mean for each donor is shown in Figure 5B to note any differences in activation between donors. Values are presented as the percentage change normalized to the DMSO control group. Kruskal-Wallis Test was performed and corrected for multiple comparisons using the Dunn's Test. ***$P < .001$. 300-500 cells (around 25-30 fields of view) were analyzed

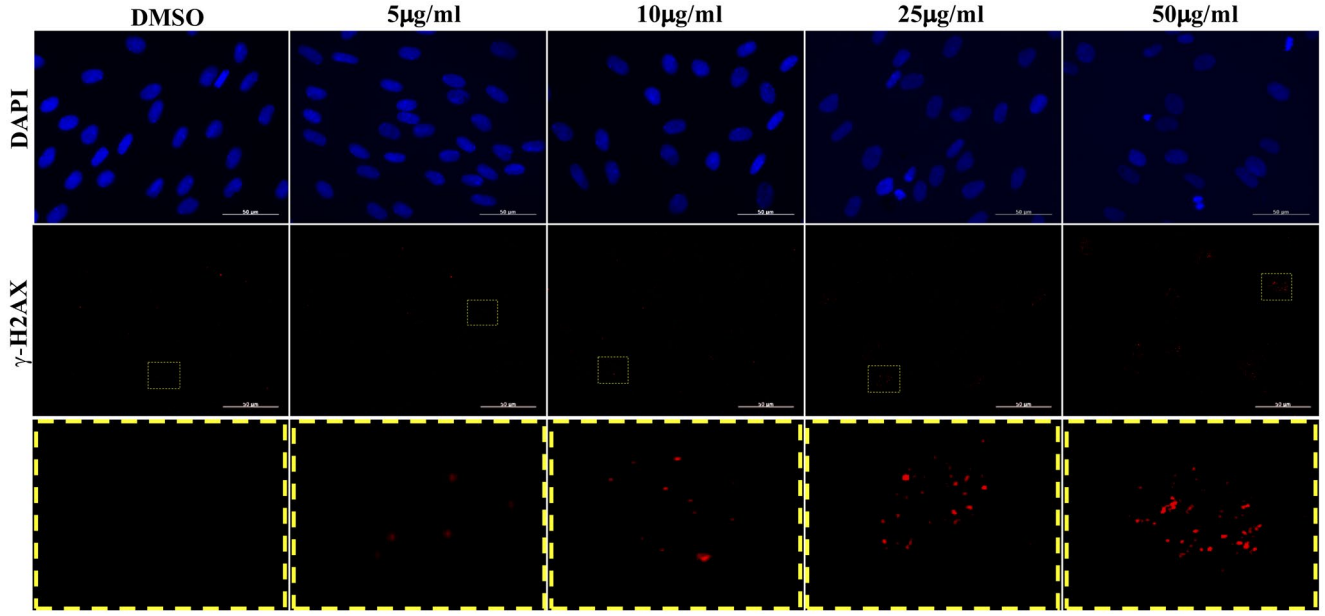

FIGURE 6 Effect of PM exposure on double strand DNA breaks in dermal fibroblasts after 24 h using γ-H2AX. Dermal fibroblasts were treated with DMSO (vehicle control) or different concentrations of PM for 24 h and fixed. Cells were then stained with anti-γ-H2AX antibody and counterstained with 4,6-diamidino-2-phenylindole (DAPI), before being visualized with fluorescence microscopy. A magnified image of γ-H2AX-stained cells is represented by a dashed, yellow box for each treatment group

blotting. Western blotting showed antibody specificity for both the active and pro-forms of each MMP, therefore, dot blotting was used to quantify total MMP expression. In the cases of both MMP-1 and MMP-3, all three donors showed no statistically significant changes in expression at 8 or 24 h, as shown in Figure 8A,B, respectively. For MMP-1 (Figure 8A), all donors showed statistically significant increases at the higher PM concentrations after 4 d of exposure, with the increases for donors two and three being very similar ($P = .0345$ and $P = .0001$ for 25 and 50 μg/mL, respectively). However, donor one showed a more substantial increase with over double the increase of either donor two or three. A mean increase of 23%, 73.4%, and 161.1% was observed for 10, 25, 50 μg/mL, respectively, after 4 d exposure between three donors. At 7 d, donors one and three showed similar increases in expression, with donor two proving to be more resilient and having a lower level of induction. After 7 d of incubation, a mean increase of 27.1%, 83.3%, and 266.2% was observed for 10, 25, 50 μg/mL, respectively ($P = .0135$ and $P = .0001$ for 25 and 50 μg/mL respectively). For MMP-3 (Figure 8B), all donors showed statistically significant increases at the higher PM concentrations at the 4 d time point, with the increases for donor one and two being very similar and donor three showing a higher level of induction. Between the three donors, total MMP-3 expression followed a mean increase of 15.2%, 20.5%, and 36.9% for 10, 25, and 50 μg/mL, respectively, after 4 d of exposure. After 7 d total MMP-3 expression followed a mean increase of 2.3%, 14.8%, and 47.2% for 10, 25, and 50 μg/mL, respectively.

3.5 | PM modulates expression of other key proteins

Antibody specificity for TGFβ was confirmed with Western blotting, before analysis of secretory TGFβ expression in dermal fibroblasts after PM treatment using dot blotting. Western blotting showed antibody specificity for only the latent forms of TGFβ, therefore, dot blotting was used to quantify inactive TGFβ expression. In all three donors, no statistically significant changes in expression were seen at 4 or 7 d.

PM dose-dependently increased latent TGFβ expression at 8 and 24 h with statistical significance at the higher PM concentrations, as shown in Figure 9. After 8 h, a decrease in latent TGFβ expression was noted, which could indicate either degradation of latent TGFβ or activation of latent TGFβ. The mean percentage increases after 8 h of exposure were 22.9%, 43.3%, and 79.5% for 10, 25, 50 μg/mL, respectively ($P = .0028$ and $P = .0001$ for 25 and 50 μg/mL respectively). After 24 h of exposure, the mean percentage increases were 3.3%, 10.8%, and 31.4% for 10, 25, 50 μg/mL, respectively ($P = .0412$ for 50 μg/mL, respectively).

4 | DISCUSSION

In the present study, the PM "urban dust" used was a compound mixture prepared from atmospheric particulate matter in the Washington, DC area. This includes a mixture of particulate matter sizes (averaging 10 μm), 23 certified PAHs, 13 polychlorinated biphenyls, 4 pesticides, and trace metals.

The AhR activation induced by this PM is more than likely due to one or multiple of the PAHs which are known to bind to AhR with different affinities.[27] The ability to activate AhR means that PM can regulate transcription and translation of enzymes that can metabolize components of PM and produce ROS. ROS not only damages DNA directly, but can also interact with activator protein 1 (AP-1) and NF-κB elements in the promoter gene regions to alter the expression of numerous proteins including cytokines and MMPs that can ultimately damage normal skin physiology.[28-30] Some of these effects can be demonstrated in this current study with not only PM-induced increases in DSBs, but also the increases in MMP-1, MMP-3, and TGFβ protein expression.

An increase in DSBs reduced the likelihood that these breaks are repaired correctly, incorrect repair can then result in cellular dysfunction, cell changes toward a senescent or oncogenic phenotype, or even cell death. After DSBs, cells initiate a DNA damage response (DDR) that detects and repairs DNA damage, this includes the PI3 kinase regulated phosphorylation of histone H2AX which is necessary for a DNA repair proteins assembly at the damaged chromatin sites.[31] It is thought that increased cellular aging correlates with increased accumulation of DSBs and the impaired capacity to repair them.[26] The dose-dependent increase in the number of DSBs caused by PM demonstrates genotoxic potential which if sustained could lead to cellular senescence, and therefore, implicate air pollution in the premature aging of human skin.

MMP expression was also seen to be influenced by PM, which can increase the signs of premature aging by degrading ECM proteins. The lack of a statistically significant increase in MMP-1 and MMP-3 expression at 8 and 24 h could be explained by an initial protective mechanism of the cell to inhibit MMP expression in order to resist damage. This theory is corroborated by a significant increase in latent TGFβ at 8 and 24 h, as TGFβ is believed to modulate the homeostasis between MMPs and their tissue inhibitors (TIMPs), with the latent form inhibiting MMP expression and the active form inducing MMP expression. This could mean the cells are trying to minimize PM-induced increases in MMP expression at the early stages of PM exposure. However, this increase declines over time, this could be due to degradation or becoming activated since the antibody only detects latent forms of TGFβ. Since ROS have been shown to activate latent TGFβ, it is possible that as the cells are continually exposed to PM the ROS level exceeds a threshold limit and activates TGFβ, which induces increased MMP expression as seen at 4 and 7 d.[32]

Extended exposures to TGFβ can lead to fibroblast-myofibroblast differentiation and excessive ECM production, these are known stages of fibrosis and can impair tissue function.[33] TGFβ can also display both proliferative and antiproliferative capacities, thought to be dependent on the concentration of the cytokine itself.[34] TGFβ-induced increases in fibroblast proliferation are thought to be due to the expression of basic fibroblast growth factor-2 (FGF-2).[35] This concentration-dependent proliferation switch may also explain why TGFβ can induce cellular senescence, with a high enough concentration arresting cell growth, inducing β-galactosidase activity, and senescence-associated gene expression.[36] TGFβ may also be the culprit for the dose-dependent increase in cell viability as well as the visual observation of increased cell number, however, there are conflicting reports as to whether increased proliferation rate is caused by latent or active TGFβ.[37,38] An alternative cause of the increased cellular viability is that the ROS produced by PM metabolism is not high enough to damage cells but enough to stimulate the cells to increase their mitochondrial number/activity in order to combat the low-level oxidative stress.

In conclusion, we demonstrated that PM has the ability to modulate the proliferation rate, induce DSBs, and activate AhR in human dermal fibroblasts. PM-induced activation

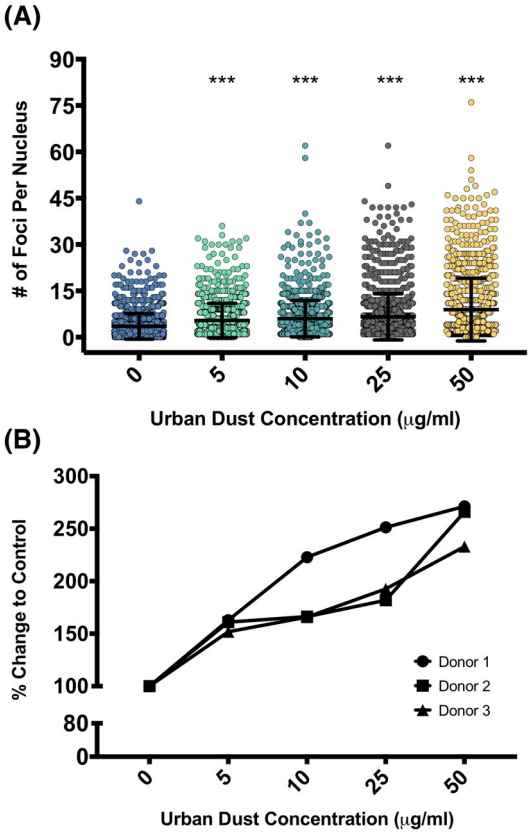

FIGURE 7 PM-induced double-strand DNA breaks. The number of phosphorylated H2AX foci in each individual cell nuclei after PM treatment for all three donors is shown in Figure 7A (n = 3). The mean for each donor is shown in Figure 7B to note any differences in double strand DNA breaks between donors. Values are presented as the percentage change normalized to the DMSO control group. Kruskal-Wallis Test was performed and corrected for multiple comparisons using the Dunnett's Test. ***$P < .001$. 300-500 cells (around 25-30 fields of view) were analyzed

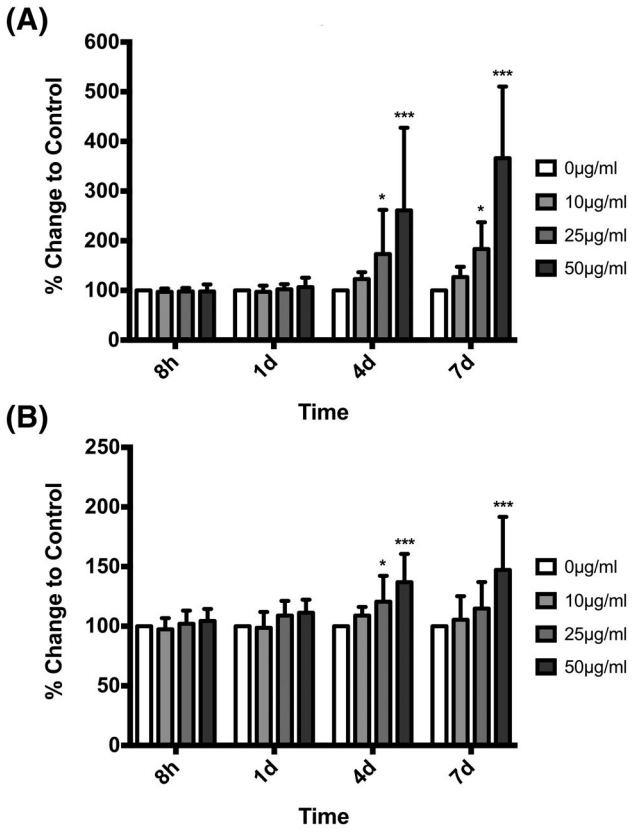

FIGURE 8 PM-induced increases in MMP secretion in dermal fibroblasts. Dot blotting was used to assess changes in MMP-1 (Figure 8A) and MMP-3 (Figure 8B) expression in dermal fibroblasts after exposure to PM. Graph shows mean + SD and is based on dermal fibroblasts isolated from three separate donors, with each donor consisting of triplicate experiments (n = 3). Values are presented as the percentage change to the DMSO control group. Two-way ANOVA was performed and corrected for multiple comparisons using the Dunnett's Test.*$P < .05$, ***$P < .001$

of AhR could then potentiate the induction of MMP-1 and MMP-3 expression seen in this study through its metabolic regulation to form ROS. Increased MMP expression could implicate air pollutants in the premature aging of human skin, given their ability to degrade ECM proteins that maintain skin integrity, such as collagen I. Even an increase in latent MMP forms can be detrimental to ECM proteins, and therefore, skin structure, with an increase in their bioavailability allowing more chance for other factors to activate them. Such activating factors include Cathepsins, which have been shown to be upregulated after exposure to UV in skin cells, this could indicate a synergistic role of pollutants in the aging of human skin.[39-41] In addition, TGFβ dysregulation can also inhibit proliferation and induce cell senescence, which can ultimately influence skin matrix composition.

With more of the damaging effects of air pollutants being discovered, this brings a pressing need for the production and use of pollution protective strategies to maintain skin integrity and function.

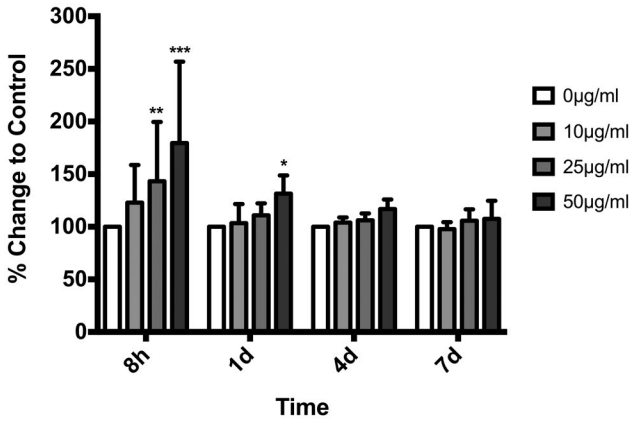

FIGURE 9 PM-induced increases in TGFβ. Dot blotting was used to assess changes in TGFβ expression in dermal fibroblasts after exposure to PM. Graph shows mean + SD and is based on dermal fibroblasts isolated from three separate donors, with each donor consisting of triplicate experiments (n = 3). Values are presented as the percentage change to the DMSO control group. Two-way ANOVA was performed and corrected for multiple comparisons using the Dunnett's Test.*$P < .05$, **$P < .01$, ***$P < .001$

ACKNOWLEDGMENTS

The work in this study was funded by UK Research and Innovation/Biotechnology and Biological Sciences Research Council (UKRI/BBSRC, BB/S506837/1) in collaboration with Croda, awarded to Mark A. Birch-Machin as principal investigator. The authors would like to thank Lina Patterson (Newcastle University, UK), Stephanie Meyer (Newcastle University, UK) for their technical assistance with the dot blotting and γ-H2AX assays, and also the Newcastle Biobank. We also thank Fang Liu-Walsh (Johnson & Johnson, USA) for scientific advice and Ayla Kiser (Johnson & Johnson, France) for comments on the manuscript. This research has been conducted following ethical approval through the Newcastle Biobank under application number #075 (17/NE/0361).

CONFLICTS OF INTEREST

The author declares no conflict of interest.

AUTHOR CONTRIBUTIONS

M.A. Birch-Machin as the senior and corresponding author co-designed the research with B. Chavan. W.J. Reynolds performed the experiments and wrote the paper. A. Critchley and B. Griffiths provided the tissue from which the cells were isolated. P.S. Hanson provided technical and experimental design support. M.A. Birch-Machin, B. Chavan, and P.S. Hanson for comments on the manuscript.

REFERENCES

1. Laing S, Wang G, Briazova T, et al. Airborne particulate matter selectively activates endoplasmic reticulum stress response in the

lung and liver tissues. *Am J Physiol Cell Physiol*. 2010;299(4):C736-C749.
2. Ruckerl R, Schneider A, Breitner S, Cyrys J, Peters A. Health effects of particulate air pollution: a review of epidemiological evidence. *Inhalation Toxicol*. 2011;23(10):555-592.
3. World Health Organization. *Ambient air pollution: A global assessment of exposure and burden of disease*. Geneva, Switzerland: World Health Organization; 2018:131.
4. Ngoc LTN, Park D, Lee Y, Lee YC. Systematic review and meta-analysis of human skin diseases due to particulate matter. *Int J Env Res Public Health*. 2017;14(12):1458.
5. Phalen RF. The particulate air pollution controversy. *Nonlinearity in Biol Toxicol Med*. 2004;2(4):259-292.
6. Vierkotter A, Schikowski T, Ranft U, et al. Airborne particle exposure and extrinsic skin aging. *J Invest Dermatol*. 2010;130(12):2719-2726.
7. Magnani ND, Muresan XM, Belmonte G, et al. Skin damage mechanisms related to airborne particulate matter exposure. *Toxicol Sci*. 2016;149(1):227-236.
8. Lademann J, Otberg N, Jacobi U, Hoffman RM, Blume-Peytavi U. Follicular penetration and targeting. *J Investig Dermatol Symp Proc*. 2005;10(3):301-303.
9. Jin SP, Li Z, Choi EK, et al. Urban particulate matter in air pollution penetrates into the barrier-disrupted skin and produces ROS-dependent cutaneous inflammatory response in vivo. *J Dermatol Sci*. 2018;91(2):175-183.
10. Rosso JD, Zeichner J, Alexis A, Cohen D, Berson D. Understanding the epidermal barrier in healthy and compromised skin: clinically relevant information for the dermatology practitioner: proceedings of an expert panel roundtable meeting. *J Clin Aesthet Dermatol*. 2016;9(4 Suppl 1):S2-S8.
11. Menichini E. Urban air pollution by polycyclic aromatic hydrocarbons: levels and sources of variability. *Sci Total Environ*. 1992;116(1–2):109-135.
12. Ruchirawat M, Settachan D, Navasumrit P, Tuntawiroon J, Autrup H. Assessment of potential cancer risk in children exposed to urban air pollution in Bangkok, Thailand. *Toxicol Lett*. 2007;168(3):200-209.
13. Koohgoli R, Hudson L, Naidoo K, Wilkinson S, Chavan B, Birch-Machin MA. Bad air gets under your skin. *Exp Dermatol*. 2017;26(5):384-387.
14. Afaq F, Zaid MA, Pelle E, et al. Aryl hydrocarbon receptor is an ozone sensor in human skin. *J Invest Dermatol*. 2009;129(10):2396-2403.
15. Mancebo SE, Wang SQ. Recognizing the impact of ambient air pollution on skin health. *J Eur Acad Dermatol Venereol*. 2015;29(12):2326-2332.
16. Hudson L, Rashdan E, Bonn CA, Chavan B, Rawlings D, Birch-Machin MA. Individual and combined effects of the infrared, visible, and ultraviolet light components of solar radiation on damage biomarkers in human skin cells. *FASEB J*. 2020;34(3):3874-3883.
17. Valacchi G, Sticozzi C, Belmonte G, et al. Vitamin C compound mixtures prevent ozone-induced oxidative damage in human keratinocytes as initial assessment of pollution protection. *PLoS One*. 2015;10(8):e0131097.
18. Beelen R, Hoek G, van den Brandt PA, et al. Long-term exposure to traffic-related air pollution and lung cancer risk. *Epidemiology*. 2008;19(5):702-710.
19. Castano-Vinyals G, Cantor KP, Malats N, et al. Air pollution and risk of urinary bladder cancer in a case-control study in Spain. *Occup Environ Med*. 2008;65(1):56-60.
20. Kadunce DP, Burr R, Gress R, Kanner R, Lyon JL, Zone JJ. Cigarette smoking: risk factor for premature facial wrinkling. *Ann Intern Med*. 1991;114(10):840-844.
21. Kim KE, Cho D, Park HJ. Air pollution and skin diseases: adverse effects of airborne particulate matter on various skin diseases. *Life Sci*. 2016;152:126-134.
22. Forecast MD. Anti-aging market by demographics, by products, by services, by devices, and by region-global industry analysis, size, share, growth, trends, and forecasts (2016–2021). *Orbis Res*. 2018;1(1):178.
23. Tigges J, Krutmann J, Fritsche E, et al. The hallmarks of fibroblast ageing. *Mech Ageing Dev*. 2014;138:26-44.
24. Bonnier F, Keating ME, Wrobel TP, et al. Cell viability assessment using the Alamar blue assay: a comparison of 2D and 3D cell culture models. *Toxicol in Vitro*. 2015;29(1):124-131.
25. Jesus RMD, Mosca AC, Guarieiro ALN, Rocha GOD, Andrade JBD. In vitro evaluation of oxidative stress caused by fine particles (PM2.5) exhausted from heavy-duty vehicles using diesel/biodiesel blends under real world conditions. *J Braz Chem Soc*. 2018;29:1268-1277.
26. Zorin V, Grekhova A, Pustovalova M, et al. Spontaneous gamma-H2AX foci in human dermal fibroblasts in relation to proliferation activity and aging. *Aging*. 2019;11(13):4536-4546.
27. Lee S, Shin WH, Hong S, et al. Measured and predicted affinities of binding and relative potencies to activate the AhR of PAHs and their alkylated analogues. *Chemosphere*. 2015;139:23-29.
28. Ono Y, Torii K, Fritsche E, et al. Role of the aryl hydrocarbon receptor in tobacco smoke extract-induced matrix metalloproteinase-1 expression. *Exp Dermatol*. 2013;22(5):349-353.
29. Tu Y, Quan T. Oxidative stress and human skin connective tissue aging. *Cosmetics*. 2016;3(3):28.
30. Pittayapruek P, Meephansan J, Prapapan O, Komine M, Ohtsuki M. Role of matrix metalloproteinases in photoaging and photocarcinogenesis. *Int J Mol Sci*. 2016;17(6):868.
31. Podhorecka M, Skladanowski A, Bozko P. H2AX phosphorylation: its role in DNA damage response and cancer therapy. *J Nucleic Acids*. 2010;2010:1-9.
32. Krstic J, Trivanovic D, Mojsilovic S, Santibanez JF. Transforming growth factor-beta and oxidative stress interplay: implications in tumorigenesis and cancer progression. *Oxidative medicine and cellular longevity*. 2015;2015:654594.
33. Chen X, Thibeault SL. Response of fibroblasts to transforming growth factor-beta1 on two-dimensional and in three-dimensional hyaluronan hydrogels. *Tissue Eng Part A*. 2012;18(23–24):2528-2538.
34. Zhang Y, Alexander PB, Wang XF. TGF-beta family signaling in the control of cell proliferation and survival. *Cold Spring Harb Perspect Biol*. 2017;9(4):1–22.
35. Strutz F, Zeisberg M, Renziehausen A, et al. TGF-beta 1 induces proliferation in human renal fibroblasts via induction of basic fibroblast growth factor (FGF-2). *Kidney Int*. 2001;59(2):579-592.
36. Debacq-Chainiaux F, Borlon C, Pascal T, et al. Repeated exposure of human skin fibroblasts to UVB at subcytotoxic level triggers premature senescence through the TGF-beta1 signaling pathway. *J Cell Sci*. 2005;118(Pt 4):743-758.
37. Campaner AB, Ferreira LM, Gragnani A, Bruder JM, Cusick JL, Morgan JR. Upregulation of TGF-beta1 expression may be

necessary but is not sufficient for excessive scarring. *J Invest Dermatol*. 2006;126(5):1168-1176.

38. Takai S, Jin D, Sakaguchi M, et al. A novel chymase inhibitor, 4-[1-([bis-(4-methyl-phenyl)-methyl]-carbamoyl)3-(2-ethoxy-benzyl)-4-oxo-azetidin e-2-yloxy]-benzoic acid (BCEAB), suppressed cardiac fibrosis in cardiomyopathic hamsters. *J Pharmacol Exp Ther*. 2003;305(1):17-23.
39. Xu QF, Zheng Y, Chen J, et al. Ultraviolet A enhances cathepsin L expression and activity via JNK pathway in human dermal fibroblasts. *Chin Med J*. 2016;129(23):2853-2860.
40. Piao MJ, Susara Ruwan Kumara MH, Kim KC, et al. Diphlorethohydroxycarmalol suppresses ultraviolet B-induced matrix metalloproteinases via inhibition of JNK and ERK signaling in human keratinocytes. *Biomol Ther*. 2015;23(6):557-563.
41. Codriansky KA, Quintanilla-Dieck MJ, Gan S, Keady M, Bhawan J, Runger TM. Intracellular degradation of elastin by cathepsin K in skin fibroblasts–a possible role in photoaging. *Photochem Photobiol*. 2009;85(6):1356-1363.

How to cite this article: Reynolds WJ, Hanson PS, Critchley A, Griffiths B, Chavan B, Birch-Machin MA. Exposing human primary dermal fibroblasts to particulate matter induces changes associated with skin aging. *The FASEB Journal*. 2020;00:1–11. https://doi.org/10.1096/fj.202001357R